East palearctic treefrog past and present habitat suitability using ecological niche models

Desiree Andersen[1], Irina Maslova[2], Zoljargal Purevdorj[3,4], Jia-Tang Li[5], Kevin R. Messenger[6], Jin-Long Ren[5], Yikweon Jang[1,7]*, Amaël Borzée[8]*

[1]Department of Life Science and Division of EcoScience, Ewha Womans University, Seoul, Republic of Korea

[2]Federal Scientific Center of the East Asia Terrestrial Biodiversity Far Eastern Branch of Russian Academy of Sciences, Vladivostock, Russian Federation

[3] Department of Biology, Scholl of Mathematic and Natural Science, Mongolian State University of Education, Ulaanbaatar 210685, Mongolia

[4] Department of Forest and Environmental Resources, Chungnam National University, Daejeon 34134, Republic of Korea

[5]Chengdu Institute of Biology, Chinese Academy of Sciences, Chengdu, People's Republic of China

[6]Nanjing Forestry University, Nanjing, People's Republic of China

[7]Interdisciplinary Program of EcoCreative, Ewha Womans University, Seodaemun Seoul, Republic of Korea

[8]Laboratory of Animal Behaviour and Conservation, College of Biology and the Environment, Nanjing Forestry University, Nanjing, People's Republic of China

Corresponding Authors:
Yikweon Jang[1,7]
52 Ewhayeodae-gil, Seodaemun-gu, Seoul, 03760, Republic of Korea
Email address: jangy@ewha.ac.kr
Amaël Borzée[8]
159 Longpan Rd, Nanjing, 210037, People's Republic of China
Email address: amaelborzee@gmail.com

Abstract

39
40 Ecological niche modeling is a tool used to determine current potential species' distribution or
41 habitat suitability models which can then be used to project suitable areas in time. Projections of
42 suitability into past climates can identify locations of climate refugia, or areas with high climatic
43 stability likely to contain the highest levels of genetic diversity and stable populations when
44 climatic conditions are less suitable in other parts of the range. Modeling habitat suitability for
45 closely related species in recent past can also reveal potential periods and regions of contact and
46 possible admixture. In the east palearctic, there are five *Dryophytes* (Hylid treefrog) currently
47 non-sympatric clades belonging to two groups: *Dryophytes japonicus* group: Clades A and B;
48 and *Dryophytes immaculatus* group: *Dryophytes immaculatus*, *Dryophytes flaviventris*, and
49 *Dryophytes suweonensis*. We used maximum entropy modeling to determine the suitable ranges
50 of these five clades during the present and projected to the Last Glacial Maximum (LGM) and
51 Last Interglacial (LIG) periods. We also calculated climatic stability for each clade to identify
52 possible areas of climate refugia. Our models indicated suitable range expansion during the LGM
53 for four clades with the exclusion of *D. immaculatus*. High climatic stability in our models
54 corresponded to areas with the highest numbers of recorded occurrences in the present. The
55 models produced here can additionally serve as baselines for models of suitability under climate
56 change scenarios and indicate species ecological requirements.
57

Introduction

59   Past distributions of species relate to patterns of current distributions, genetics (Carnaval
60 et al., 2009), and biodiversity hotspots (Carnaval & Moritz, 2008; Woodruff, 2010; Tang et al.,
61 2018) and can therefore inform conservation practices. For example, recent genetic analysis of
62 Floreana's lizards (*Microlophus*) in the Galapagos supports the hypothesis of "glaciation driven
63 contact" between conspecifics where Floreana and Champion islands were connected during the
64 Pleistocene glacial maximum, and therefore Champion Island may be a source for potential
65 reintroduction of *Microlophus* to Floreana Island in the event of extinction since they are
66 genetically similar (Torres-Carvajal, Castaño & Moreno, 2021). Similarly, in a study of endemic
67 plants in East Asia, paleogeographic models showed that areas with high climatic suitability in
68 the mid Holocene and last glacial maximum correlated to high levels of endemism in the present,
69 meaning those areas provide long-term stable refugia for relict plant species (Tang et al., 2018).
70   Climatic stability may indicate areas of climate refugia (Gavin et al., 2014) where a
71 species has been extant consistently across shifting climatic conditions. These areas can harbor
72 the highest levels of species' genetic diversity and are therefore principally important for
73 conservation (Loera, Ickert-Bond & Sosa, 2017). Identifying areas of high genetic diversity is
74 important for species conservation as genetic diversity promotes adaptation and long-term
75 survival of the metapopulation (Booy et al., 2000; Vandewoestijne, Schtickzelle & Baguette,
76 2008), particularly in microrefugial populations (Mosblech, Bush & van Woesik, 2011). Climatic
77 stability can also be used to identify areas that would remain suitable for species in different
78 climate change scenarios, which will become vital for persistence of species at risk of extinction

79   (Ashcroft, 2010; Keppel et al., 2012; Morelli et al., 2016). This is especially true for amphibians
80   due to the current extinction crisis in the class (Beebee & Griffiths, 2005; Sodhi et al., 2008;
81   Wake & Vredenburg, 2008). For example, climate change models of a plethodontid salamander
82   (*Karsenia koreana*) in the Republic of Korea predicted a near total shift in suitable climate for
83   the species under moderate to severe climate change scenarios, wherein the species' current
84   range would be almost completely outside of the suitable range predicted in the future (Borzée et
85   al., 2019a).
86   Ecological niche models, also called species distribution or habitat suitability models,
87   represent the presence probability or abundance of species, usually using environmental
88   predictor variables (Guisan & Zimmermann, 2000; Guisan & Thuiller, 2005; Elith & Leathwick,
89   2009; Guisan, Thuiller & Zimmermann, 2017). These models can be easily projected across
90   geographic ranges and time scales and can therefore be valuable to climate change and
91   paleogeographic research. Such models are particularly useful for species that do not disperse
92   over long distances, such as amphibians which generally have continuous distribution patterns
93   (Duellman, 1999) and do not disperse over long distances (Smith & Green, 2005). In
94   amphibians, paleogeographic suitability models combined with genetic analysis have linked
95   Malagasy bullfrog (*Laliostoma labrosum*) divergence with periods of high aridity during the
96   Pleistocene (Pabijan et al., 2015).
97   In the east palearctic (encompassing northeast Asia), treefrogs in the genus *Dryophytes*
98   face ongoing threats such as habitat loss (Borzée et al., 2015, 2017a; Kuzmin et al., 2017;
99   Borzée, 2020), drought (Kuzmin et al., 2017), pollution (Borzée et al., 2018), invasive species
100   (Wu et al., 2005), disease (Borzée et al., 2017b) and competition (Borzée et al., 2016; Borzée,
101   Kim & Jang, 2016). Among these, habitat loss is considered the biggest risk to the clade, as
102   suitable habitat is converted from artificial wetland (rice paddies) to other forms of agriculture
103   (Kuzmin et al., 2017). Additionally, climate change is expected to negatively impact amphibian
104   species worldwide (Blaustein et al., 2001; Corn, 2005; Lips et al., 2008; Struecker & Milanovich,
105   2017).
106   The objectives of the current study were to model present and past habitat suitability and
107   stability for five east palearctic *Dryophytes* clades: two clades of *D. japonicus*, *D. immaculatus*,
108   *D. flaviventris* and *D. suweonensis*. To model present and past habitat suitability, we utilized the
109   maximum entropy algorithm (MaxEnt; Phillips et al., 2017) because of its ability to easily create
110   ecological niche models that can be projected to past or future climate scenarios. In creating
111   suitability and stability models for these five clades, we aim to also identify areas of potential
112   climatic refugia and determine climatic preferences for all clades.
113

Materials & Methods

115   *Focal species*
116   There are currently four recognized species of *Dryophytes* in the east palearctic: *D.*
117   *japonicus*, *D. immaculatus*, *D. flaviventris* and *D. suweonensis*. *Dryophytes japonicus* is split
118   into two clades (hereafter Clades A and B) with the Clade A being found in Japan northeast of

119 the Chugoku-Kansai border (Dufresnes et al., 2016) and Clade B, likely associated with the
120 name *Hyla stepheni* (Dufresnes et al., 2016; Borzée et al., 2020b), is found widely across
121 mainland northeast Asia and Japan southwest of the Chugoku-Kansai border (Dufresnes et al.,
122 2016). *Dryophytes immaculatus*, *D. flaviventris*, and *D. suweonensis* are combined into the
123 *Dryophytes immaculatus* group, with *D. immaculatus* found in mainland China, *D. suweonensis*
124 found in the Republic of Korea and the Democratic People's Republic of Korea, north of the
125 Chilgap mountains, and *D. flaviventris* found in the Republic of Korea south of the Chilgap
126 mountains and north of the Mangyeong river (Borzée et al., 2020b). The species within the *D.*
127 *immaculatus* clade are generally restricted to the low elevation alluvial plains around the Yellow
128 sea (Borzée et al., 2020b) while *D. japonicus* is found at variable elevation, breeding in a variety
129 of water bodies (Tsuji et al., 2011; Roh, Borzée & Jang, 2014; Borzée et al., 2019b), and human
130 alteration of the landscape resulted in hybridization between the two groups (Borzée et al.,
131 2020a).
132 *Climatic suitability modelling and projection to past climates*
133   We used maximum entropy (MaxEnt ver. 3.4.4; Elith et al., 2011; Phillips et al., 2017)
134 modelling to predict present and past distributions of *Dryophytes* in the east palearctic,
135 separating the *Dryophytes japonicus* group into two clades (called A and B in Dufresnes et al.,
136 2016) and the *Dryophytes immaculatus* group into three species (*D. flaviventris*, *D. immaculatus*
137 and *D. suweonensis*; Borzée et al., 2020b). Occurrences were obtained from the Global
138 Biodiversity Information Facility (GBIF.org, 2021) and non-focal surveys and opportunistic
139 observations conducted by the authors (Supplementary file). In filtering GBIF data, we removed
140 occurrences with more than 4000 m accuracy, which was the cell size of the environmental
141 layers used to train our models. We omitted occurrences by the National Institute of Ecology
142 Korea (NIEK) since the methodology used by the institute (gridded sampling along transects)
143 differed from other data sources and led to uneven sampling which overestimated common
144 species (*D. japonicus*) while underestimating rare species (*D. flaviventris* and *D. suweonensis*).
145 To further reduce sampling bias, we reduced the occurrences of *D. japonicus* in the Republic of
146 Korea to 20% using the "Subset" tool in ArcMap 10.8.1 (ESRI, Redlands, CA, USA). We finally
147 removed occurrence points of *D. japonicus* along the Chugoku-Kansai border since the lineage
148 could ambiguously belong to either clade A or B of the species.
149   When running MaxEnt, we used seven environmental layers (Table 1) with a 2.5 arc-
150 minute (0.0417 decimal degree or ~4 km) resolution. This resolution was used as it was the
151 smallest scale available for the Last Glacial Maximum downscaled climate reconstruction. We
152 used seven independent bioclimatic variables (WorldClim 1.4; Hijmans et al., 2005) with low
153 multicollinearity (Pearson's $r < 0.8$) which were previously determined to influence present and
154 past distributions of *D. japonicus* in the east palearctic (Dufresnes et al., 2016). We opted to only
155 use climatic variables and exclude terrain variables that potentially correlate to present-day
156 distributions (Borzée et al., 2020b) as current topography (e.g., elevation) may not correlate to
157 the same climatic conditions across geologic time scales (Peterson et al., 2011; Jarnevich et al.,
158 2015; Bobrowski et al., 2021). For example, other species have been predicted to shift their

159   elevational distribution as a result of past climate change (Yousefi et al., 2015). For model
160   replication, we used the cross-validate run type option with five replicates (5 k-fold), which uses
161   80% of occurrences for training and 20% for testing. We selected the option to remove duplicate
162   presence points within the same cell of the environmental layers. To address overfitting
163   (Radosavljevic & Anderson, 2014), we created models at three levels of background points
164   (5000, 10000, 15000) and four levels of randomization multipliers (0.5, 1.0, 1.5, 2.0). We finally
165   projected our trained models to past climates of the last glacial maximum (LGM; 22 kya;
166   WorldClim 1.4; Hijmans et al., 2005) and last interglacial (LIG; 130 kya; WorldClim 1.4; Otto-
167   Bliesner et al., 2006). For our climate projected models, we ran multivariate environmental
168   similarity surface (MESS) analysis (Elith, Kearney & Phillips, 2010) to identify areas of novel
169   past climates with no modern analog where a projected climate suitability model may require
170   more careful interpretation. For each model, we calculated the area under the curve (AUC) for
171   training and test data, true skill statistic (TSS; Allouche et al., 2006), and percent omission of test
172   data for minimum and 10 percent omission thresholds. TSS was calculated from MaxEnt output
173   test and background model values by (from Allouche et al., 2006):

174

175   $$Sensitivity = \frac{a}{a + c}$$

176

177   $$Specificity = \frac{d}{b + d}$$

178
179   $$TSS = Sensitivity + Specificity - 1$$

180
181   Where:
182   a = number of occurrences (test points) for which presence was correctly predicted by the model
183   b = number of occurrences (background points) for which the species was not found but the model
184   predicted presence
185   c = number of occurrences (test points) for which the species was found but the model predicted absence
186   d = number of occurrences (background points) for which absence was correctly predicted by the model
187
188   We additionally calculated the difference between training and test AUC for each model.
189   We selected best models for each clade based on these fit statistics, choosing models with low
190   difference between training and test AUC, minimum test omission closest to 0% and 10 percent
191   test omission closest to 10% (or below). To calculate the area of suitability for each clade, we
192   thresholded the models at the maximum test sensitivity plus specificity threshold (true scale
193   statistic or TSS; Allouche et al., 2006), a threshold which maximizes true presences and absences
194   while minimizing false presences and absences. Finally, to visualize areas of potential climatic
195   refugia, we used the "Cell Statistics" tool (specifying "sum" as the overlay statistics) in ArcMap
196   10.8.1 (ESRI, Redlands, CA, USA) to create stability models for each clade by calculating the

197 sum of cloglog outcomes of our suitability models across time periods (Loera, Ickert-Bond &
198 Sosa, 2017).
199
200

Results

202 *Model evaluation*
203   Models for all clades produced AUC values greater than 0.9 (Table 2), which is
204 considered excellent fit (Dolgener et al., 2014). Models for the *D. japonicus* Clade B (TSS =
205 0.8077), *D. immaculatus* (TSS = 0.7946) and *D. flaviventris* (TSS = 0.8329) had very good
206 presence-absence prediction capability while models for the *D. japonicus* Clade A (TSS =
207 0.9475) and *D. suweonensis* (TSS = 0.9127) had almost perfect presence-absence prediction
208 capability (Table 2). See Supplementary Figures S1-S5 for all tested models and statistics.
209 *Present and past distributions and areas*
210   The *D. japonicus* Clade A had a similar suitable range (defined here as the thresholded
211 area of suitability) during the last interglacial (LIG) to its current suitable range (Figure 1).
212 During the last glacial maximum (LGM), its suitable range shifted south and contracted in the
213 northern part of its current suitable range, with a disjunct suitable range in the Yellow Sea Basin
214 and mainland China. The *D. japonicus* Clade B also shifted south during the LGM with a LIG
215 suitable range similar to its current suitable range in mainland northeast Asia and southern Japan
216 (Figure 2). Both *D. japonicus* clades experienced expansion from the LIG to the LGM, and then
217 subsequent detraction in the present (Table 3). *Dryophytes immaculatus* experienced suitable
218 range contraction from the LIG to the LGM, but an expansion from the LGM to the present
219 (Figure 3). *Dryophytes flaviventris* experienced a suitable range detraction across all three time
220 periods, becoming the clade with the smallest suitable range in the present at 10,760 km^2. The
221 clade's suitable range in the LIG covered large patches in China and the Korean peninsula and
222 had a large area of suitability in the Yellow Sea Basin during the LGM (Figure 4). *Dryophytes*
223 *suweonensis* experienced a marked increase in suitable range from the LIG to the LGM (29,480
224 km^2 to 816,268 km^2) mostly in the Yellow Sea Basin (Figure 5), but in the present its suitable
225 range is similar to its LIG suitable range.
226   For *D. japonicus* Clade A, the highest climatic stability areas were in lowland and coastal
227 areas of central Japan (Figure 1), while the highest climatic stability for *D. japonicus* Clade B
228 occurred in the Korean peninsula and southern Japan (Figure 2). For *D. immaculatus*, high
229 climatic stability was found along the Yangtze River (Figure 3). High climatic stability for *D.*
230 *flaviventris* was limited to coastal lowlands in the southwestern corner of South Korea (Figure
231 4). Climatic stability for *D. suweonensis* occurred in the lowlands of the western Korean
232 peninsula, with a small area of stability along the eastern coast of the Democratic People's
233 Republic of Korea around the city of Wonsan (Figure 5).
234   MESS analysis was similar for all clades, with a small area of novel climatic conditions
235 during the LGM in the north and a larger area during the LIG mostly in present-day China
236 (Figures 1-5, S6). During the LGM, the main novel limiting climatic variables were Bio1, Bio2

237 and Bio3. During the LIG, the main novel limiting climatic variables for all clades were Bio2,
238 Bio5 and Bio15.

239 *Variable importance*

240   The variables contributing the most to the distribution of the *D. japonicus* Clade A was
241 Bio19 (precipitation of coldest quarter) at 49.69% (Table 4), while Bio15 (precipitation
242 seasonality) had the highest permutation importance at 84.36% (Table 5). For the *D. japonicus*
243 Clade B, elevation was the highest for both percent contribution and permutation importance.
244 Elevation was also the highest variable for *D. flaviventris*, with a contribution of 68.19% and
245 permutation importance of 67.30%. The variable with highest contribution (37.36%) and
246 permutation importance (48.88%) for *D. immaculatus* was Bio1 (annual mean temperature). For
247 *D. suweonensis*, elevation had the highest percent contribution at 36.56%, while Bio12 (annual
248 precipitation) had the highest permutation at 76.68%.

249

250 ## Discussion

251 *Habitat suitability and stability*

252   The highest stability areas for the two *D. japonicus* clades match their current respective
253 ranges. For the *D. japonicus* Clade A, this range is in central Japan. The highest stability areas
254 for the *D. japonicus* Clade B are in the Korean peninsula, between Vladivostok and Khabarovsk
255 along the Ussuri River, and in southern Japan. Comparison with previous research (Dufresnes et
256 al., 2016) suggests a possible correlation between high stability areas and a greater number of
257 haplotypes of *Dryophytes japonicus* clades in the Korean peninsula and southern Japan. Future
258 research may find a significant correlation between climatic stability and genetic diversity for the
259 two clades. There is also moderately stable area in mainland China west of the Yellow Sea,
260 which makes it surprising that the clade is not found in this region. This may simply be because
261 the species did not disperse to the area while it was accessible, or competition with *D.*
262 *immaculatus* or another species (Borzée et al., 2016; Borzée, Kim & Jang, 2016) may have
263 prevented expansion.

264   High stability areas for *D. immaculatus* follow the Yellow River Basin where the species
265 is most prevalent. *Dryophytes flaviventris* has high stability areas in its current range as well as
266 an area south of its range (South Jeolla province of Rep. of Korea). As the species is declining
267 and facing continued habitat destruction, translocation to the South Jeolla province of Rep. of
268 Korea may aid conservation efforts. Additionally, since there is high stability in two coastal areas
269 of Shandong and Hebei, molecular tools or call analysis may be needed to confirm the species in
270 those areas. The highest stability areas for *D. suweonensis* also match with its current known
271 range with the exception of a high stability area along the east coast of the Democratic People's
272 Republic of Korea. However, as the species has not been recorded in the area and is
273 geographically isolated from the known range, it is unlikely the species occurs there.

274   During the LGM, all clades had suitable area in the then-exposed Yellow Sea Basin. This
275 would have allowed for contact and created a situation where admixture was possible. As
276 previous research has estimated the divergence time between *D. immaculatus* and the *D.*

277   *suweonensis* group at around 1.02 mya (Borzée et al., 2020b), it is possible that a minor
278   glaciation during this time (Ehlers, Gibbard & Hughes, 2018) saw the clades splitting from a
279   shared range in the Yellow Sea Basin. However, the merging of all the rivers into the Yellow Sea
280   Basin may have created a barrier that was too difficult for Hylids to cross as observed by the
281   Vistula River segregation of *Hyla arborea* and *Hyla orientalis* in Poland (Stöck et al., 2012) and
282   in the Middle East where the Dead Sea Rift has divided *Hyla savignyi* and *Hyla felixarabica*
283   (Dufresnes et al., 2019).

284   Range expansions for the *D. japonicus* clades, *D. flaviventris* and *D. suweonensis* during
285   the LGM are in line with previous studies which have seen LGM expansion in a temperate hylid
286   *Hyla sarda* (Bisconti et al., 2011). Cooler temperatures that would allow temperate species
287   expansion might have also limited the LGM range of *D. immaculatus* which is currently found at
288   lower latitudes and more subtropical climates.

289   *Variable responses and species ecology*

290   Variables having the highest percent contribution and/or permutation importance in
291   ecological models indicate potential preference or limiting factors for species. For the *D.*
292   *japonicus* Clade A, these variables included precipitation of coldest quarter and precipitation
293   seasonality. Since the region is generally marked by dry winters, this shows a preference towards
294   wetter winters and less precipitation variability between seasons (Figure 6). This is interesting
295   because a similar preference is not seen in Clade B. Instead, elevation is the variable with the
296   highest contribution and importance, with the species found at low elevations mostly between 0
297   and 400 meters (Figure 6). Elevation was similarly important for *D. flaviventris* and *D.*
298   *suweonensis*, whose cloglog responses both peak around sea level (0 m). This fits with the
299   species' habitat preferences for alluvial plains and makes the species particularly vulnerable to
300   sea level rise. For *D. suweonensis*, the high permutation importance of annual precipitation
301   indicates a preference for moderate annual rainfall with a tolerance for higher rainfall better than
302   lower rainfall and peaking at 1240 mm. Finally, for *D. immaculatus*, there is a preference for
303   higher annual mean temperature, which relates largely to its range as the clade present at the
304   lowest latitudes.

305   Ecological niche modeling also allows for among-species comparisons in responses to
306   environmental variables. Interestingly, annual mean temperature for all clades peaked between
307   10 to 16 °C indicating preference for warmer climates, with the *D. japonicus* Clade B tolerating
308   cooler temperatures likely in its northern range in Russia. Maximum temperature of warmest
309   month peaks below 35 °C for all clades likely because of critical thermal limits. A study of
310   another hylid, *Dryophytes versicolor*, showed a decrease in tadpole speed past about 32 °C with
311   a sharp decrease occurring around 34 °C (Katzenberger et al., 2014).

312

313   **Conclusions**

314   Because of the numerous threats facing *Dryophytes* treefrogs in the east palearctic, it is
315   important to determine their ecological requirements in order to implement conservation plans
316   (Park, Park & Borzée, 2021). By using modeling, we have mapped areas of likely refugia,

317 identified areas for potential translocation and determined regional-scale climatic and terrain
318 requirements for five clades of endangered or otherwise at-risk treefrogs in the east palearctic.
319 Additionally, we have provided a baseline for modeling habitat suitability for these clades in
320 future climates under mild to extreme climate change scenarios.
321

Acknowledgements

323 YJ was funded by the research grants from the Rural Development Administration of Korea
324 (PJ015071022021) and from the Korea Environmental Industry & Technology Institute (KEITI
325 2021002270001).
326

327

328

References

330 Allouche O, Tsoar A, Kadmon R. 2006. Assessing the accuracy of species distribution models:

331 prevalence, kappa and the true skill statistic (TSS). *Journal of Applied Ecology* 43:1223–

332 1232.

333 Ashcroft MB. 2010. Identifying refugia from climate change. *Journal of Biogeography* 37:1407–

334 1413. DOI: https://doi.org/10.1111/j.1365-2699.2010.02300.x.

335 Beebee TJ, Griffiths RA. 2005. The amphibian decline crisis: a watershed for conservation

336 biology? *Biological Conservation* 125:271–285.

337 Bisconti R, Canestrelli D, Colangelo P, Nascetti G. 2011. Multiple lines of evidence for

338 demographic and range expansion of a temperate species (*Hyla sarda*) during the last

339 glaciation. *Molecular Ecology* 20:5313–5327.

340 Blaustein AR, Belden LK, Olson DH, Green DM, Root TL, Kiesecker JM. 2001. Amphibian

341 Breeding and Climate Change. *Conservation Biology* 15:1804–1809. DOI:

342 https://doi.org/10.1046/j.1523-1739.2001.00307.x.

343 Bobrowski M, Weidinger J, Schwab N, Schickhoff U. 2021. Searching for ecology in species

344 distribution models in the Himalayas. *Ecological Modelling* 458:109693. DOI:

345 10.1016/j.ecolmodel.2021.109693.

346   Booy G, Hendriks RJJ, Smulders MJM, Groenendael JMV, Vosman B. 2000. Genetic Diversity

347   and the Survival of Populations. *Plant Biology* 2:379–395. DOI: https://doi.org/10.1055/s-

348   2000-5958.

349   Borzée A. 2020. Recommendations for IUCN Red List Conservation Status of the "*Dryophytes*

350   *immaculatus* Group" in North East Asia. *Diversity* 12:336. DOI: 10.3390/d12090336.

351   Borzée A, Ahn J, Kim S, Heo K, Jang Y. 2015. Seoul, keep your paddies! Implications for the

352   conservation of hylid species. *Animal Systematics, Evolution and Diversity* 31:176–181.

353   Borzée A, Andersen D, Groffen J, Kim H-T, Bae Y, Jang Y. 2019a. Climate change-based

354   models predict range shifts in the distribution of the only Asian plethodontid salamander:

355   *Karsenia koreana*. *Scientific Reports* 9:1–9. DOI: 10.1038/s41598-019-48310-1.

356   Borzée A, Fong JJ, Nguyen HQ, Jang Y. 2020a. Large-scale hybridisation as an extinction

357   threat to the Suweon treefrog (Hylidae: *Dryophytes suweonensis*). *Animals* 10:764.

358   Borzée A, Kim JY, Cunha MAMD, Lee D, Sin E, Oh S, Yi Y, Jang Y. 2016. Temporal and spatial

359   differentiation in microhabitat use: Implications for reproductive isolation and ecological

360   niche specification. *Integrative Zoology* 11:375–387. DOI: https://doi.org/10.1111/1749-

361   4877.12200.

362   Borzée A, Kim K, Heo K, Jablonski PG, Jang Y. 2017a. Impact of land reclamation and

363   agricultural water regime on the distribution and conservation status of the endangered

364   *Dryophytes suweonensis*. *PeerJ* 5:e3872.

365   Borzée A, Kim JY, Jang Y. 2016. Asymmetric competition over calling sites in two closely

366   related treefrog species. *Scientific Reports* 6:1–12.

367   Borzée A, Kosch TA, Kim M, Jang Y. 2017b. Introduced bullfrogs are associated with increased

368   *Batrachochytrium dendrobatidis* prevalence and reduced occurrence of Korean

369   treefrogs. *PLoS One* 12:e0177860. DOI: 10.1371/journal.pone.0177860.

370   Borzée A, Kyong CN, Kil HK, Jang Y. 2018. Impact of water quality on the occurrence of two

371   endangered Korean anurans: *Dryophytes suweonensis* and *Pelophylax chosenicus*.

372   *Herpetologica* 74:1–7.

373   Borzée A, Messenger KR, Chae S, Andersen D, Groffen J, Kim YI, An J, Othman SN, Ri K,

374   Nam TY. 2020b. Yellow sea mediated segregation between North East Asian

375   *Dryophytes* species. *PLoS One* 15:e0234299.

376   Borzée A, Purevdorj Z, Kim YI, Kong S, Choe M, Yi Y, Kim K, Kim A, Jang Y. 2019b. Breeding

377   preferences in the treefrogs *Dryophytes japonicus* (Hylidae) in Mongolia. *Journal of*

378   *Natural History* 53:2685–2698.

379   Carnaval AC, Hickerson MJ, Haddad CFB, Rodrigues MT, Moritz C. 2009. Stability Predicts

380   Genetic Diversity in the Brazilian Atlantic Forest Hotspot. *Science* 323:785–789. DOI:

381   10.1126/science.1166955.

382   Carnaval AC, Moritz C. 2008. Historical climate modelling predicts patterns of current

383   biodiversity in the Brazilian Atlantic forest. *Journal of Biogeography* 35:1187–1201.

384   Corn PS. 2005. Climate change and amphibians. *Animal Biodiversity and Conservation* 28:59–

385   67.

386   Dolgener N, Freudenberger L, Schluck M, Schneeweiss N, Ibisch PL, Tiedemann R. 2014.

387   Environmental niche factor analysis (ENFA) relates environmental parameters to

388   abundance and genetic diversity in an endangered amphibian, the fire-bellied-toad

389   (*Bombina bombina*). *Conservation Genetics* 15:11–21.

390   Duellman WE. 1999. *Patterns of distribution of amphibians: a global perspective*. JHU Press.

391   Dufresnes C, Litvinchuk SN, Borzée A, Jang Y, Li J-T, Miura I, Perrin N, Stöck M. 2016.

392   Phylogeography reveals an ancient cryptic radiation in East-Asian tree frogs (*Hyla*

393   *japonica* group) and complex relationships between continental and island lineages.

394   *BMC Evolutionary Biology* 16:253. DOI: 10.1186/s12862-016-0814-x.

395   Dufresnes C, Mazepa G, Jablonski D, Sadek RA, Litvinchuk SN. 2019. A river runs through it:

396   tree frog genomics supports the Dead Sea Rift as a rare phylogeographical break.

397   *Biological Journal of the Linnean Society* 128:130–137. DOI: 10.1093/biolinnean/blz076.

398   Ehlers J, Gibbard PL, Hughes PD. 2018. Chapter 4 - Quaternary Glaciations and Chronology.

399   In: Menzies J, van der Meer JJM eds. *Past Glacial Environments (Second Edition)*.

400   Elsevier, 77–101. DOI: 10.1016/B978-0-08-100524-8.00003-8.

401   Elith J, Kearney M, Phillips S. 2010. The art of modelling range-shifting species. *Methods in*

402   *ecology and evolution* 1:330–342.

403   Elith J, Leathwick JR. 2009. Species distribution models: ecological explanation and prediction

404   across space and time. *Annual review of ecology, evolution, and systematics* 40:677–

405   697.

406   Elith J, Phillips SJ, Hastie T, Dudík M, Chee YE, Yates CJ. 2011. A statistical explanation of

407   MaxEnt for ecologists. *Diversity and distributions* 17:43–57.

408   Gavin DG, Fitzpatrick MC, Gugger PF, Heath KD, Rodríguez-Sánchez F, Dobrowski SZ, Hampe

409   A, Hu FS, Ashcroft MB, Bartlein PJ, Blois JL, Carstens BC, Davis EB, Lafontaine G de,

410   Edwards ME, Fernandez M, Henne PD, Herring EM, Holden ZA, Kong W, Liu J, Magri

411   D, Matzke NJ, McGlone MS, Saltré F, Stigall AL, Tsai Y-HE, Williams JW. 2014. Climate

412   refugia: joint inference from fossil records, species distribution models and

413   phylogeography. *New Phytologist* 204:37–54. DOI: https://doi.org/10.1111/nph.12929.

414   GBIF.org. 2021. GBIF Occurrence Download. DOI: 10.15468/dl.f55u3k.

415   Guisan A, Thuiller W. 2005. Predicting species distribution: offering more than simple habitat

416   models. *Ecology letters* 8:993–1009.

417   Guisan A, Thuiller W, Zimmermann NE. 2017. *Habitat Suitability and Distribution Models: With*

418   *Applications in R*. Cambridge University Press.

419   Guisan A, Zimmermann NE. 2000. Predictive habitat distribution models in ecology. *Ecological*

420   *modelling* 135:147–186.

421   Hijmans RJ, Cameron SE, Parra JL, Jones PG, Jarvis A. 2005. Very high resolution interpolated

422   climate surfaces for global land areas. *International journal of climatology* 25:1965–1978.

423   DOI: 10.1002/joc.1276.

424   Jarnevich CS, Stohlgren TJ, Kumar S, Morisette JT, Holcombe TR. 2015. Caveats for

425   correlative species distribution modeling. *Ecological Informatics* 29:6–15. DOI:

426   10.1016/j.ecoinf.2015.06.007.

427   Katzenberger M, Hammond J, Duarte H, Tejedo M, Calabuig C, Relyea RA. 2014. Swimming

428   with predators and pesticides: how environmental stressors affect the thermal physiology

429   of tadpoles. *PLoS One* 9:e98265. DOI: 10.1371/journal.pone.0098265.

430   Keppel G, Niel KPV, Wardell-Johnson GW, Yates CJ, Byrne M, Mucina L, Schut AGT, Hopper

431   SD, Franklin SE. 2012. Refugia: identifying and understanding safe havens for

432   biodiversity under climate change. *Global Ecology and Biogeography* 21:393–404. DOI:

433   https://doi.org/10.1111/j.1466-8238.2011.00686.x.

434   Kuzmin S, Maslova I, Matsui M, Liang F, Kaneko Y. 2017. Dryophytes japonicus*. The IUCN Red*

435   *List of Threatened Species 2017: e. T55519A112714533*.

436   Lips KR, Diffendorfer J, Mendelson III JR, Sears MW. 2008. Riding the wave: reconciling the

437   roles of disease and climate change in amphibian declines. *PLoS Biology* 6:e72.

438   Lobo JM, Jiménez-Valverde A, Real R. 2008. AUC: a misleading measure of the performance of

439   predictive distribution models. *Global ecology and Biogeography* 17:145–151.

440   Loera I, Ickert-Bond SM, Sosa V. 2017. Pleistocene refugia in the Chihuahuan Desert: the

441   phylogeographic and demographic history of the gymnosperm *Ephedra compacta*.

442   *Journal of Biogeography* 44:2706–2716.

443   Morelli TL, Daly C, Dobrowski SZ, Dulen DM, Ebersole JL, Jackson ST, Lundquist JD, Millar CI,

444   Maher SP, Monahan WB, Nydick KR, Redmond KT, Sawyer SC, Stock S, Beissinger

445   SR. 2016. Managing Climate Change Refugia for Climate Adaptation. *PLoS One*

446   11:e0159909. DOI: 10.1371/journal.pone.0159909.

447 Mosblech NAS, Bush MB, van Woesik R. 2011. On metapopulations and microrefugia:

448   palaeoecological insights. *Journal of Biogeography* 38:419–429. DOI: 10.1111/j.1365-

449   2699.2010.02436.x.

450 Otto-Bliesner BL, Marshall SJ, Overpeck JT, Miller GH, Hu A. 2006. Simulating Arctic Climate

451   Warmth and Icefield Retreat in the Last Interglaciation. *Science* 311:1751. DOI:

452   10.1126/science.1120808.

453 Pabijan M, Brown JL, Chan LM, Rakotondravony HA, Raselimanana AP, Yoder AD, Glaw F,

454   Vences M. 2015. Phylogeography of the arid-adapted Malagasy bullfrog, *Laliostoma*

455   *labrosum*, influenced by past connectivity and habitat stability. *Molecular Phylogenetics*

456   *and Evolution* 92:11–24. DOI: 10.1016/j.ympev.2015.05.018.

457 Park I-K, Park D, Borzée A. 2021. Defining conservation requirements for the Suweon Treefrog

458   (*Dryophytes suweonensis*) using species distribution models. *Diversity* 13:69. DOI:

459   10.3390/d13020069.

460 Peterson AT, Soberón J, Pearson RG, Anderson RP, Martínez-Meyer E, Nakamura M, Araújo

461   MB. 2011. *Ecological Niches and Geographic Distributions*. Princeton University Press.

462   DOI: 10.1515/9781400840670.

463 Phillips SJ, Anderson RP, Dudík M, Schapire RE, Blair ME. 2017. Opening the black box: an

464   open-source release of Maxent. *Ecography* 40:887–893. DOI: 10.1111/ecog.03049.

465 Radosavljevic A, Anderson RP. 2014. Making better Maxent models of species distributions:

466   complexity, overfitting and evaluation. *Journal of Biogeography* 41:629–643. DOI:

467   10.1111/jbi.12227.

468 Roh G, Borzée A, Jang Y. 2014. Spatiotemporal distributions and habitat characteristics of the

469   endangered treefrog, *Hyla suweonensis*, in relation to sympatric *H. japonica*. *Ecological*

470   *Informatics* 24:78–84.

471   Smith AM, Green DM. 2005. Dispersal and the metapopulation paradigm in amphibian ecology

472   and conservation: are all amphibian populations metapopulations? *Ecography* 28:110–

473   128. DOI: 10.1111/j.0906-7590.2005.04042.x.

474   Sodhi NS, Bickford D, Diesmos AC, Lee TM, Koh LP, Brook BW, Sekercioglu CH, Bradshaw

475   CJ. 2008. Measuring the meltdown: drivers of global amphibian extinction and decline.

476   *PLoS One* 3:e1636.

477   Stöck M, Dufresnes C, Litvinchuk SN, Lymberakis P, Biollay S, Berroneau M, Borzée A, Ghali

478   K, Ogielska M, Perrin N. 2012. Cryptic diversity among Western Palearctic tree frogs:

479   postglacial range expansion, range limits, and secondary contacts of three European

480   tree frog lineages (*Hyla arborea* group). *Molecular Phylogenetics and Evolution* 65:1–9.

481   Struecker BP, Milanovich JR. 2017. Predicted Suitable Habitat Declines for Midwestern United

482   States Amphibians Under Future Climate and Land-Use Change Scenarios.

483   *Herpetological Conservation and Biology* 12.

484   Tang CQ, Matsui T, Ohashi H, Dong Y-F, Momohara A, Herrando-Moraira S, Qian S, Yang Y,

485   Ohsawa M, Luu HT, Grote PJ, Krestov PV, Ben LePage, Werger M, Robertson K,

486   Hobohm C, Wang C-Y, Peng M-C, Chen X, Wang H-C, Su W-H, Zhou R, Li S, He L-Y,

487   Yan K, Zhu M-Y, Hu J, Yang R-H, Li W-J, Tomita M, Wu Z-L, Yan H-Z, Zhang G-F, He

488   H, Yi S-R, Gong H, Song K, Song D, Li X-S, Zhang Z-Y, Han P-B, Shen L-Q, Huang D-

489   S, Luo K, López-Pujol J. 2018. Identifying long-term stable refugia for relict plant species

490   in East Asia. *Nature Communications* 9:4488. DOI: 10.1038/s41467-018-06837-3.

491   Torres-Carvajal O, Castaño PA, Moreno F. 2021. Comparative Phylogeography of Floreana's

492   Lizards Supports Galápagos Pleistocene Paleogeographical Model and Informs

493   Conservation Management Decisions. *Journal of Herpetology* 55:285–291.

494   Tsuji M, Ushimaru A, Osawa T, Mitsuhashi H. 2011. Paddy-associated frog declines via

495   urbanization: A test of the dispersal-dependent-decline hypothesis. *Landscape and*

496   *Urban Planning* 103:318–325. DOI: 10.1016/j.landurbplan.2011.08.005.

497   Vandewoestijne S, Schtickzelle N, Baguette M. 2008. Positive correlation between genetic

498   diversity and fitness in a large, well-connected metapopulation. *BMC Biology* 6:46. DOI:

499   10.1186/1741-7007-6-46.

500   Wake DB, Vredenburg VT. 2008. Are we in the midst of the sixth mass extinction? A view from

501   the world of amphibians. *Proceedings of the National Academy of Sciences* 105:11466–

502   11473.

503   Woodruff DS. 2010. Biogeography and conservation in Southeast Asia: how 2.7 million years of

504   repeated environmental fluctuations affect today's patterns and the future of the

505   remaining refugial-phase biodiversity. *Biodiversity and Conservation* 19:919–941. DOI:

506   10.1007/s10531-010-9783-3.

507   Wu Z, Li Y, Wang Y, Adams MJ. 2005. Diet of introduced Bullfrogs (*Rana catesbeiana*):

508   predation on and diet overlap with native frogs on Daishan Island, China. *Journal of

509   Herpetology* 39:668–674.

510   Yousefi M, Ahmadi M, Nourani E, Behrooz R, Rajabizadeh M, Geniez P, Kaboli M. 2015.

511   Upward Altitudinal Shifts in Habitat Suitability of Mountain Vipers since the Last Glacial

512   Maximum. *PLOS ONE* 10:e0138087. DOI: 10.1371/journal.pone.0138087.

513

Figure 1

Past and present predicted distribution of *Dryophytes japonicus* Clade A.

Landscape suitability for *Dryophytes japonicus* Clade A in the present, last glacial maximum (LGM), and last interglacial (LIG) periods. Past projections are overlaid with multivariate environmental similarity surface (MESS) analysis results representing novel climates with no present-day analog. Habitat stability shows areas with most consistently stable suitable climate for the species over the 130 thousand year period.
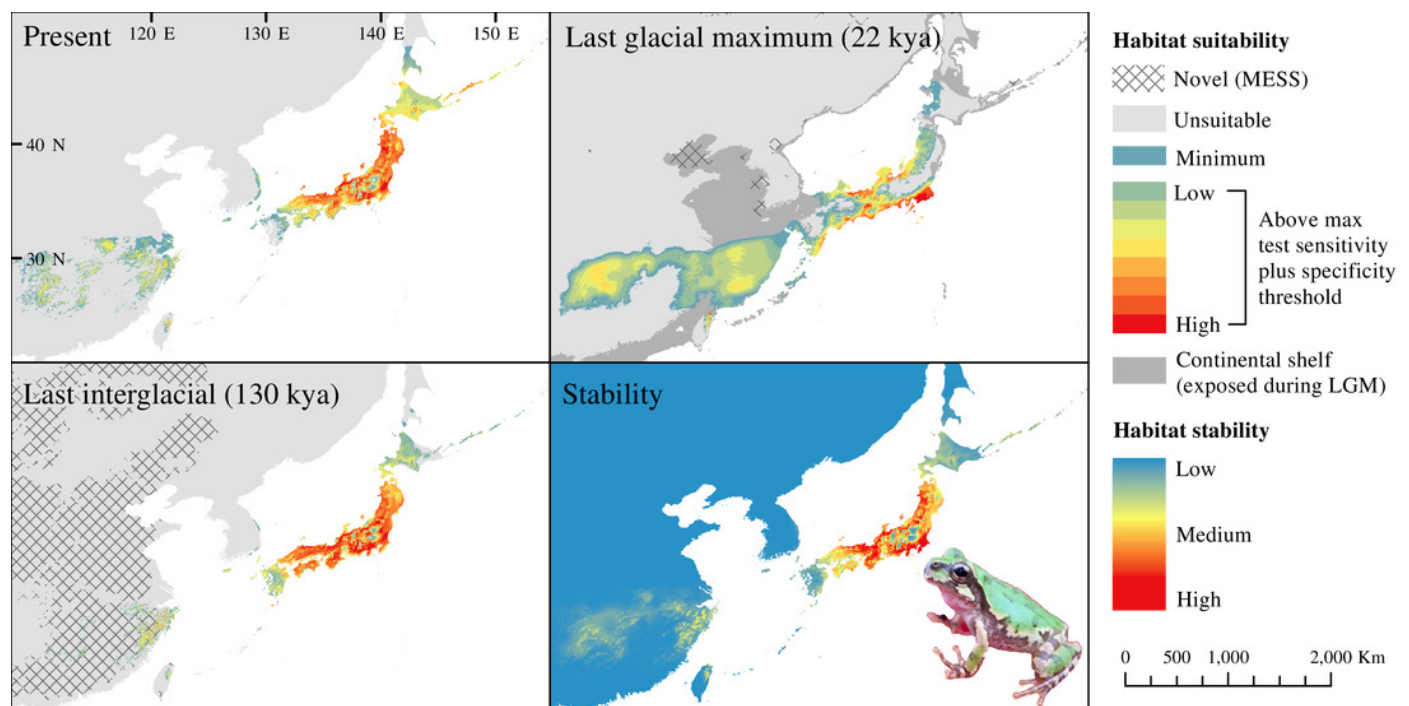
Figure 2

Past and present predicted distribution of *Dryophytes japonicus* Clade B.

Landscape suitability for *Dryophytes japonicus* Clade B in the present, last glacial maximum (LGM), and last interglacial (LIG) periods. Past projections are overlaid with multivariate environmental similarity surface (MESS) analysis results representing novel climates with no present-day analog. Habitat stability shows areas with most consistently stable suitable climate for the species over the 130 thousand year period.
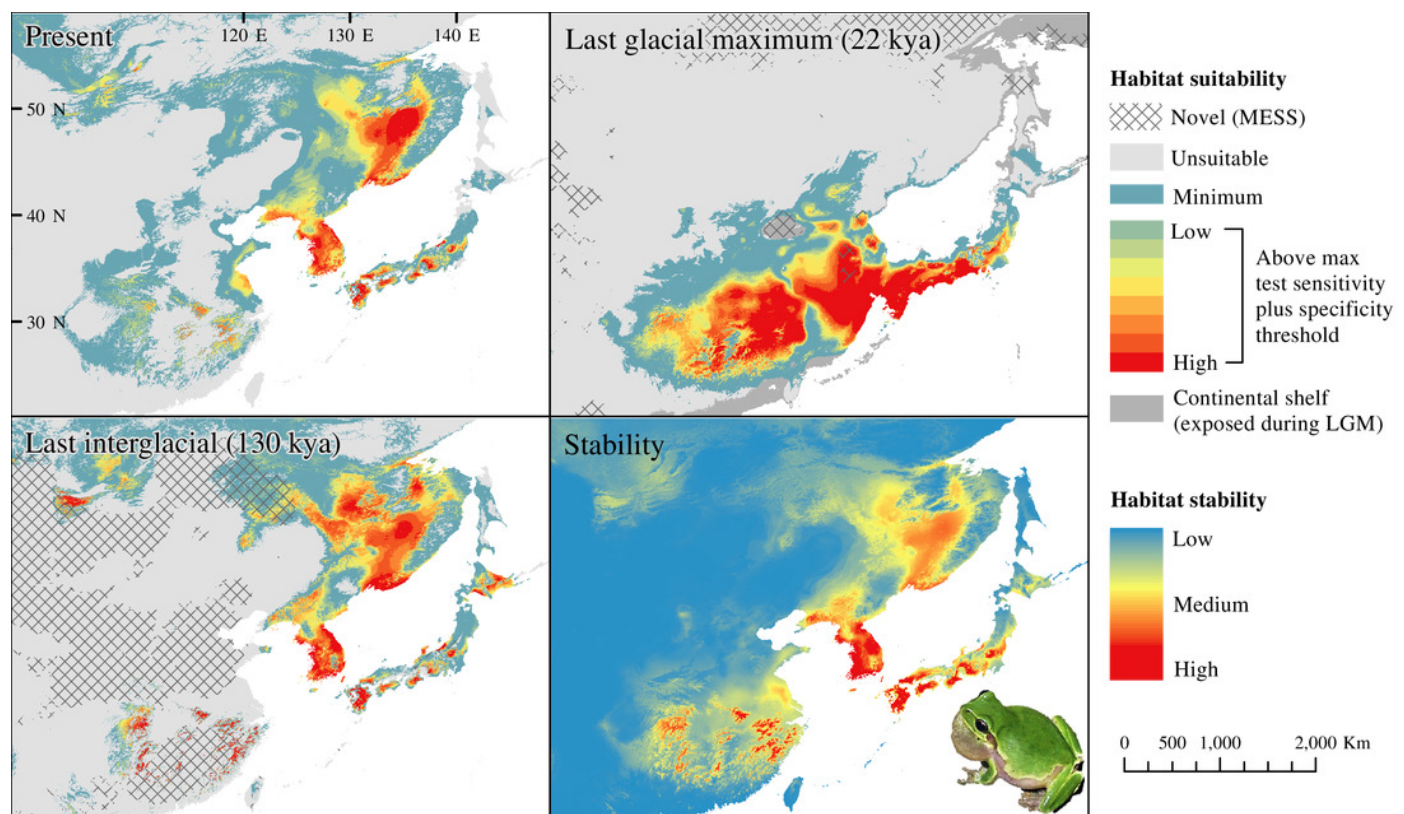
Figure 3

Past and present predicted distribution of *Dryophytes immaculatus*.

Landscape suitability for *Dryophytes immaculatus* in the present, last glacial maximum (LGM), and last interglacial (LIG) periods. Past projections are overlaid with multivariate environmental similarity surface (MESS) analysis results representing novel climates with no present-day analog. Habitat stability shows areas with most consistently stable suitable climate for the species over the 130 thousand year period.
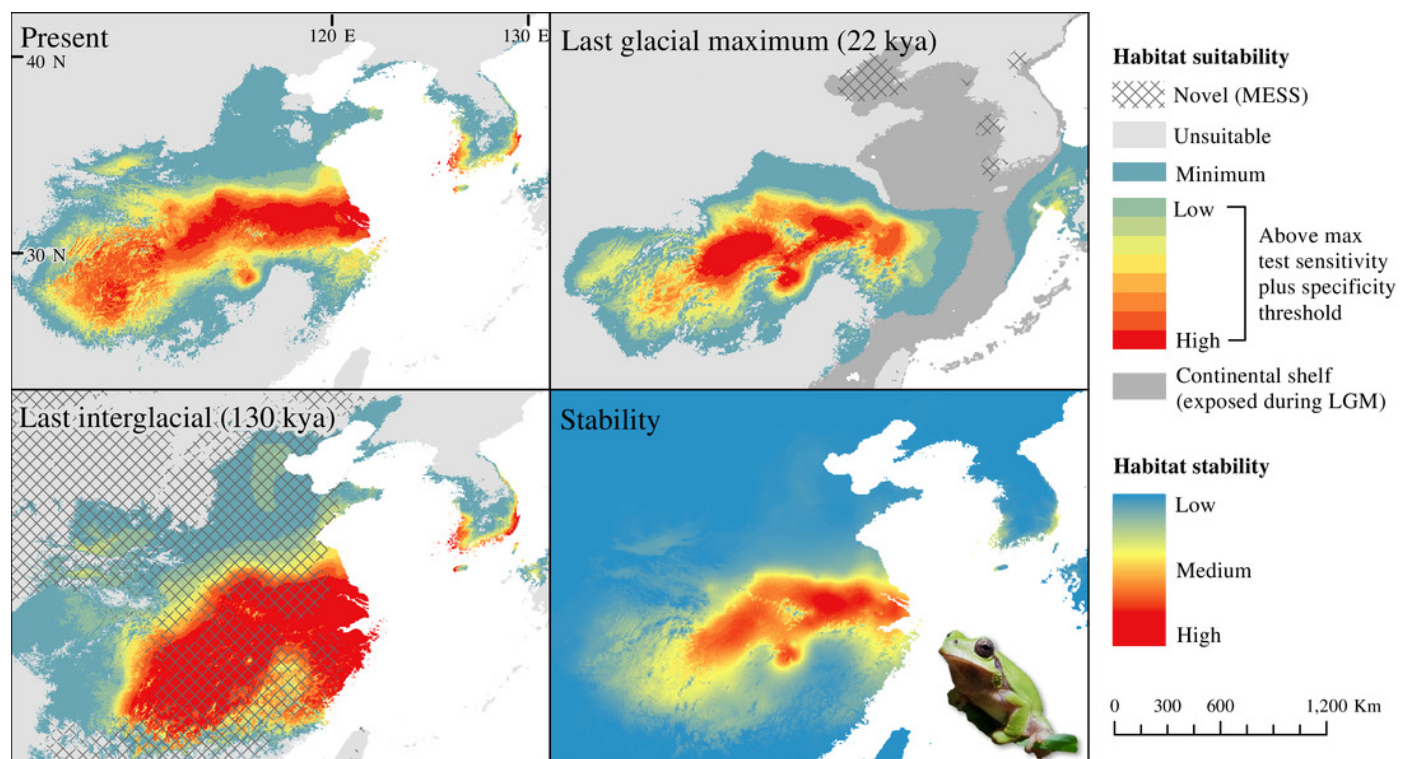
Figure 4

Past and present predicted distribution of *Dryophytes flaviventris*.

Landscape suitability for *Dryophytes flaviventris* in the present, last glacial maximum (LGM), and last interglacial (LIG) periods. Past projections are overlaid with multivariate environmental similarity surface (MESS) analysis results representing novel climates with no present-day analog. Habitat stability shows areas with most consistently stable suitable climate for the species over the 130 thousand year period.
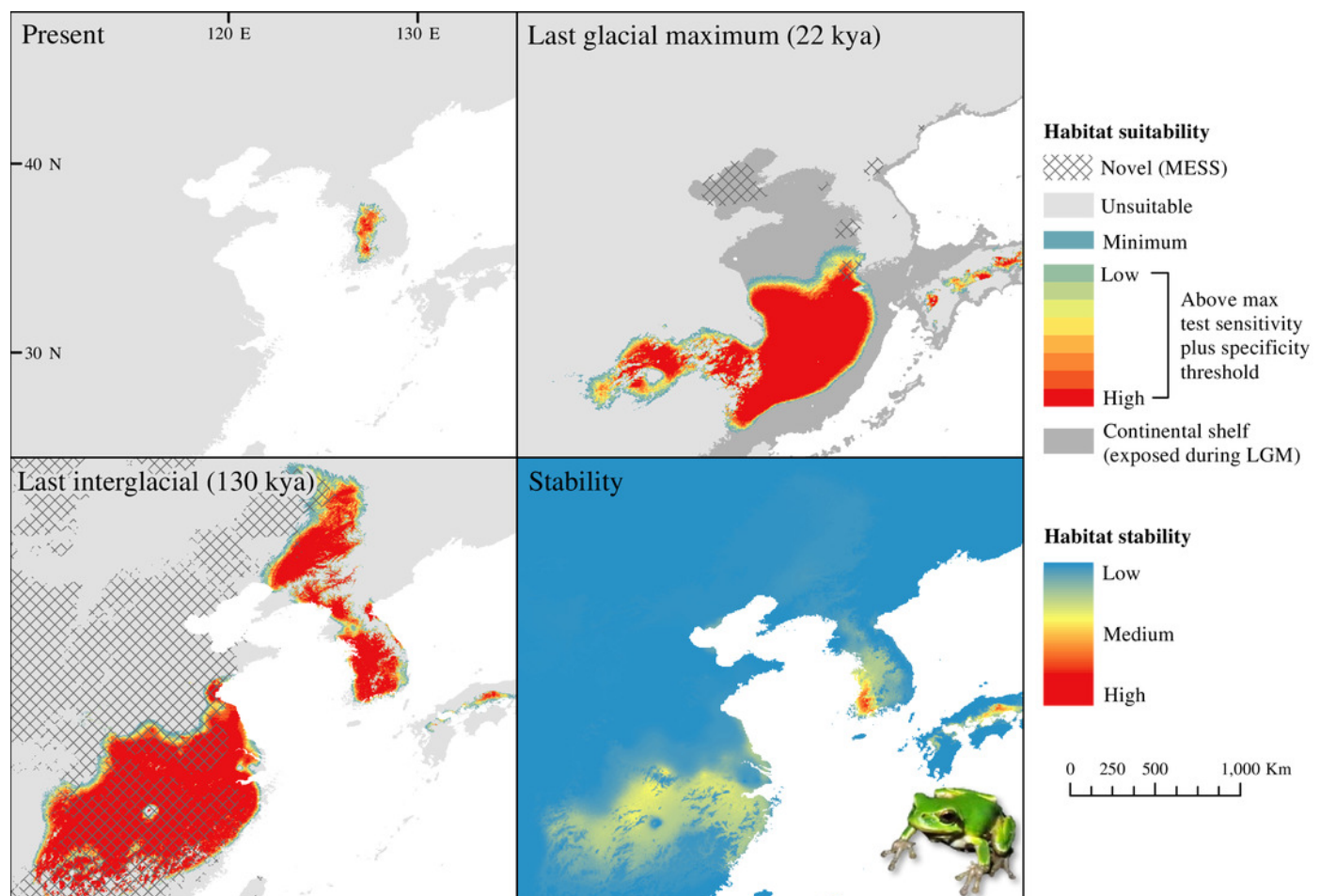
Figure 5

Past and present predicted distribution of *Dryophytes suweonensis*.

Landscape suitability for *Dryophytes suweonensis* in the present, last glacial maximum (LGM), and last interglacial (LIG) periods. Past projections are overlaid with multivariate environmental similarity surface (MESS) analysis results representing novel climates with no present-day analog. Habitat stability shows areas with most consistently stable suitable climate for the species over the 130 thousand year period.
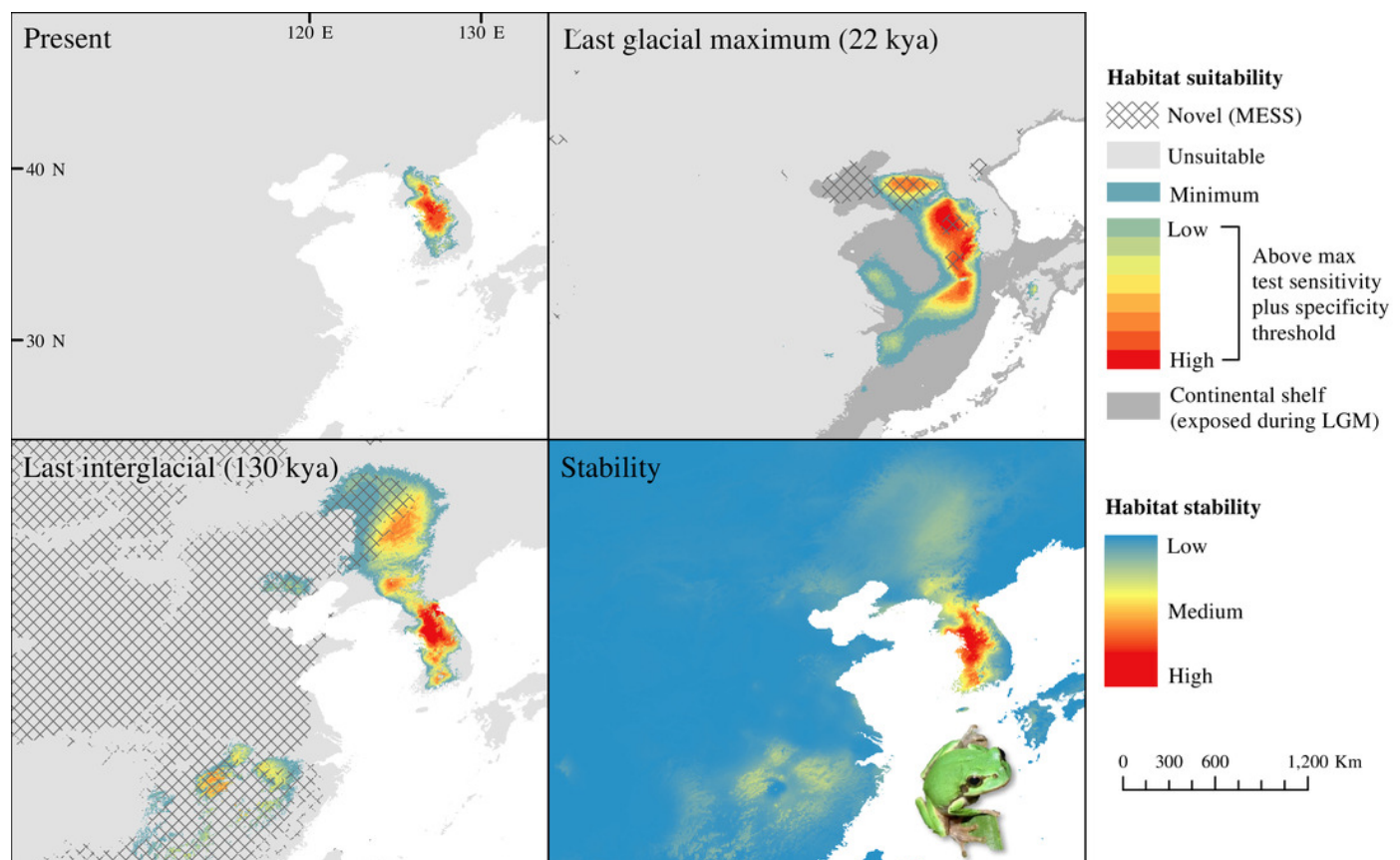
Figure 6

Bioclimatic variable response curves for *Dryophytes* clades.

Bioclimatic variable response curves for the *Dryophytes japonicus* Clades A and B, *D. flaviventris*, *D. immaculatus* and *D. suweonensis* from maximum entropy models. Responses of each variable are independent of other variables in the models.

— *Dryophytes japonicus* (Clade A)
— *Dryophytes japonicus* (Clade B)
— Dryophytes immaculatus
— *Dryophytes flaviventris*
— *Dryophytes suweonensis*
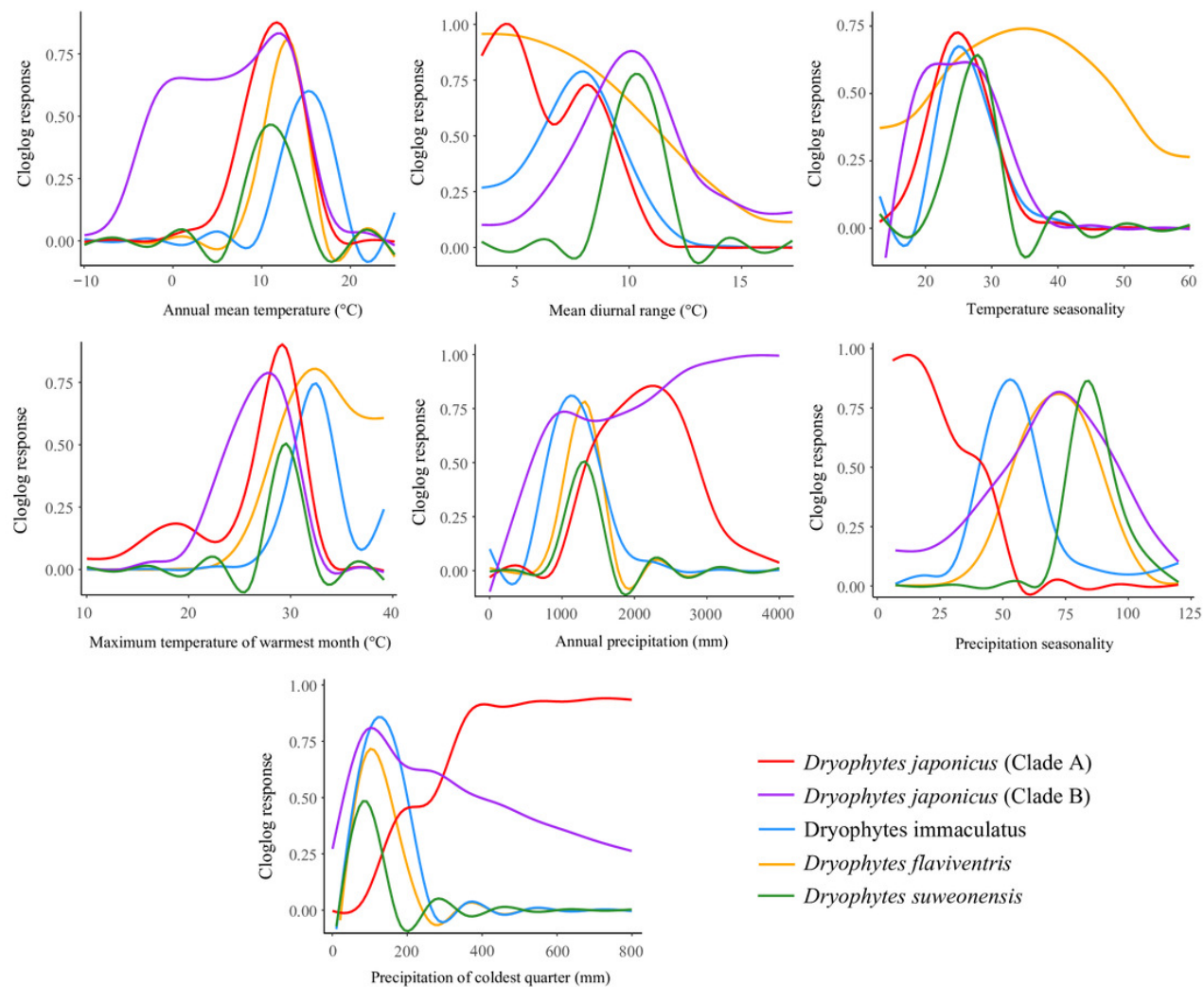
Variables used to train MaxEnt models.

Bioclimatic variables used to build maximum entropy models for five east palearctic
Dryophytes clades.

Variable	Description
Bio1	Annual mean temperature (°C)
Bio2	Mean diurnal range (°C)
Bio3	Isothermality
Bio5	Maximum temperature of warmest month (°C)
Bio12	Annual precipitation (mm)
Bio15	Precipitation seasonality
Bio19	Precipitation of coldest quarter (mm)

Model fit statistics.

Parameters and fit statistics (training and test AUC and TSS) for selected maximum entropy models of five east palearctic *Dryophytes* clades.

Clade	Randomization multiplier	Background points	Training AUC	Test AUC	TSS
Dryophytes japonicus (Clade A)	1.5	5000	0.9652 ± 0.0034	0.9644	0.9415 ± 0.0050
Dryophytes japonicus (Clade B)	1.5	10000	0.9226 ± 0.0101	0.9182	0.7438 ± 0.0453
Dryophytes immaculatus	1.5	15000	0.9707 ± 0.0093	0.9632	0.8150 ± 0.0520
Dryophytes flaviventris	2	15000	0.9985 ± 0.0004	0.9984	0.9970 ± 0.0004
Dryophytes suweonensis	2	5000	0.9910 ± 0.0016	0.9908	0.9820 ± 0.0209

Past and present estimated suitable range area.

Current estimated range and suitable area (above TSS threshold) based on selectd maximum entropy models for five east palearctic *Dryophytes* clades during the present (0 kya), last glacial maximum (22 kya) and last interglacial (~130 kya).

Clade	Current range (km²)	Suitability (km²)		
		Present	Last glacial maximum	Last interglacial
Dryophytes japonicus (Clade A)	330,726	537,358	913,731	404,657
Dryophytes japonicus (Clade B)	958,089	1,475,930	2,411,214	1,614,949
Dryophytes immaculatus	226,005	1,125,246	873,279	1,470,012
Dryophytes flaviventris	945	24,840	637,791	1,149,654
Dryophytes suweonensis	7,853	57,713	270,458	370,161

Percent contribution of environmental variables.

Variable percent contribution from selected maximum entropy models of *Dryophytes* clades in the east palearctic. Variables contributing at least 10% to the total model are bolded. See Table 1 for variable explanations.

Clade	Bio1	Bio2	Bio3	Bio5	Bio12	Bio15	Bio19
Dryophytes japonicus (Japanese)	9.29	0.42	0.23	2.50	0.31	**14.74**	**72.51**
Dryophytes japonicus (Mainland)	**24.73**	2.68	**10.73**	**21.00**	6.87	5.10	**28.90**
Dryophytes immaculatus	**48.27**	2.68	2.29	4.31	2.35	3.87	**36.22**
Dryophytes flaviventris	**31.36**	0.12	0.06	**18.90**	**32.50**	4.22	**12.85**
Dryophytes suweonensis	**19.01**	0.03	0.01	6.11	**41.40**	**17.02**	**16.42**

Permutation importance of environmental variables.

Variable permutation importance from selected maximum entropy models of *Dryophytes* clades in the east palearctic. Variables contributing at least 10% to the total model are bolded. See Table 1 for variable explanations.

Clade	Bio1	Bio2	Bio3	Bio5	Bio12	Bio15	Bio19
Dryophytes japonicus (Japanese)	8.47	0.75	0.22	0.56	4.02	**80.92**	5.06
Dryophytes japonicus (Mainland)	**26.41**	3.70	9.20	**18.47**	7.26	4.78	**30.20**
Dryophytes immaculatus	**67.91**	2.81	3.74	8.37	1.20	**10.01**	5.97
Dryophytes flaviventris	**32.60**	0.01	0.00	**51.53**	**14.39**	0.53	0.94
Dryophytes suweonensis	**21.89**	0.14	0.00	**48.74**	**14.91**	7.94	6.37